Technical Sciences
Academy of Romania
www.jesi.astr.ro

Journal of Engineering Sciences and Innovation
Volume 5, Issue 4 / 2020, p. 287 - 298
http://doi.org/10.56958/jesi.2020.5.4.287

A. Mechanical Engineering

Received ***12 August 2020*** *Accepted* ***12 November 2020***
Received in revised from ***16 October 2020***

Element-Free Galerkin Method and Finite Element Method. Which is better?

NĂSTĂSESCU VASILE[1*], ILIESCU NICOLAE[2], MARZAVAN SILVIA[1]

[1]Military Technical Academy, Bd. George Coșbuc, 81-83, S. 5, Bucharest, 050141, Romania
[2]„Politehnica" University of Bucharest, Splaiul Independenței 313, S. 6, Bucharest, 060042, Romania

Abstract*:* This paper is dedicated to the presentation of some qualities of a meshfree method – Element-Free Galerkin Method (EFGM) – which is few known and fewer used in Romania. In spite of a large using of the Finite Element Method (FEM), new numerical methods appeared, among these the Element-Free Galerkin Method (EFGM) is one. This method belongs to the meshfree methods, which is based on an approximation method named mooving least square method (MLSM). This paper presents in a synthetically way the base principle of EFGM. Some results of our researching work are also presented, which demonstrate some basic advantages of the EFGM. A simple problem of structure analysis is presented but the results are obtained by three methods: theoretical, FEM and EFGM. The results are a pleading and a model for using the EFGM. The answer of the title question is going to be given by any user of the EFGM.

Keywords: mooving least square method, element-free Galerkin, meshfree, meshless.

1. Introduction

Not many years ago, rather recently, the interest of the specialists was focused on the development of the next generation of computational methods — meshfree and meshless methods, which are expected to be superior to the conventional grid-based FEM for many circumstances and even applications.
The key idea of the meshfree methods is to provide accurate and stable numerical solutions for integral equations or partial differential equations (PDEs) with all kinds of possible boundary conditions with a set of arbitrarily distributed nodes (or particles) without using any mesh that provides the connectivity of these nodes or particles. [2] A Meshfree method is a method used to establish system algebraic

[*]Correspondence address: nastasescuv@gmail.com

equations for the whole problem domain without the use of a predefined mesh for the domain discretization [2].
Making a difference between interpolation and approximation, we must notice that by interpolation procedures, the exact values of the approximated function at the nodes are reproduced, as long as by approximation procedures, the exact values of the approximated function at the nodes are not reproduced [2].
The formulation of an equation set, by one or other numerical method can be made in a strong or weak form. In a strong-form formulation, the approximate unknown function (e.g. u, v etc.) should have enough degree of consistency, so that it is differentiable up to the order of the partial differential equations.
Obtaining the exact solution, by a strong-form formulation of an equation system is ideal, but often very difficult. In a weak-form formulation, the approximate unknown function (e.g. u, v etc.) has a weaker consistency, by introducing an integral operation to the system equations based on a mathematical or physical principle. As the weak-form formulation is based on global or local domain, we must distinguish between global or local weak-forms. From this point of view, the EFG method (EFGM) is a global weak-form method.

2. Fundamentals of the EFGM

The Element-free Galerkin method uses the moving least-squares approximation of a function $u(x)$ representing a field variable. The approximated value of $u(x)$ will be denoted by $u^h(x)$ defined by expression:

$$u^h(x) = \sum_{i=1}^{n} H_i(x) \cdot b_i(x) \tag{1}$$

In a matrix form, relation (1) is written:

$$u^h(x) = \mathrm{H}^{\mathrm{T}}(\mathrm{x})\mathrm{b}(\mathrm{x}) \tag{2}$$

where n is the order of the completeness in this approximation, the monomial $H_i(x)$ are basis functions and $b_i(x)$ are the coefficients of the approximation function.

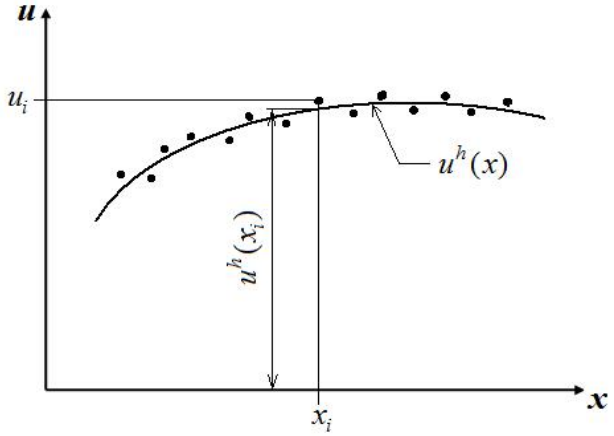

Fig. 1. Nodal parameters u_i and approximate function $u^h(x_i)$.

As the Figure 1 shows, in the moving least-squares approximation it is a difference between nodal parameter and its approximated value for a node i. The coefficients $b_i(x)$ for a point **x** depend on the sampling points $\mathbf{x_I}$ which are selected by a weighting function w_a (**x-x**$_\mathbf{I}$). A weighting function is defined on a compact support defined by a sub-domain. Each sub-domain Ω_I is associated with a node I. Often a such sub-domain is a circle or a ball (3D space), like in the Figure 2.

The moving least-squares technique is based on minimizing the weighted L_2-Norm (J) defined by the relation (3) or (4); NP is the number of nodes (points) within the support domain where $w_a(\mathbf{x}\text{-}\mathbf{x_I}) \neq 0$.

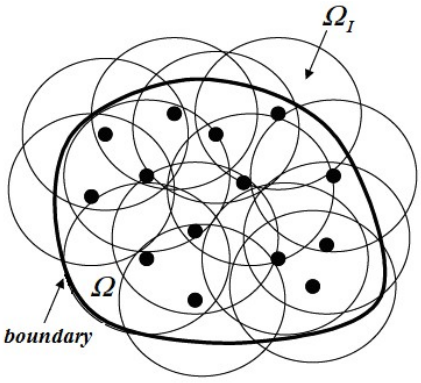

Fig. 2. A mesh-free discretization.

$$J = \sum_{I=1}^{NP} W_a(x)(x - x_I)\left[u^h(x) - u_i(x_I)\right]^2 \tag{3}$$

$$J = (\mathbf{Hb} - \mathbf{u})^{\mathrm{T}} \mathrm{W_a}(\mathbf{x})(\mathbf{Hb} - \mathbf{u}) \tag{4}$$

In the relations (3) and (4) the following notations were used:

$$\mathbf{u}^{\mathrm{T}} = (u_1, u_2, ..., u_{NP}) \tag{5}$$

$$\mathbf{H} = \begin{bmatrix} \{\mathrm{H}(\mathrm{x}_1)\}^{\mathrm{T}} \\ ... \\ \{\mathrm{H}(\mathrm{x}_{\mathrm{NP}})\}^{\mathrm{T}} \end{bmatrix} \tag{6}$$

$$\{\mathrm{H}(\mathrm{x_i})\}^{\mathrm{T}} = \{\mathrm{H_1}(\mathrm{x_i}), ..., \mathrm{H_n}(\mathrm{x_i})\} \tag{7}$$

$$\mathrm{W_a} = \mathrm{diag}\left[\mathrm{w_a}(\mathrm{x} - \mathrm{x}_1), ..., \mathrm{w_a}(\mathrm{x} - \mathrm{x}_{\mathrm{NP}})\right] \tag{8}$$

The coefficients **b** result from equation:

$$\frac{\partial \mathrm{J}}{\partial \mathrm{b}} = \mathrm{M}^{[\mathrm{n}]}(\mathrm{x})\mathrm{b}(\mathrm{x}) - \mathrm{B}(\mathrm{x})\mathrm{u} = 0 \tag{9}$$

where,

$$\mathrm{M}^{[\mathrm{n}]}(\mathrm{x}) = \mathrm{H}^{\mathrm{T}}\mathrm{W_a}(\mathrm{x})\mathrm{H} \tag{10}$$

$$\mathrm{B}(\mathrm{x}) = \mathrm{H}^{\mathrm{T}}\mathrm{W_a}(\mathrm{x}) \tag{11}$$

resulting:

$$\mathrm{b}(\mathrm{x}) = \mathrm{M}^{[\mathrm{n}]^{-1}}(\mathrm{x})\mathrm{B}(\mathrm{x})\mathrm{u} \tag{12}$$

Using the solution of the equations (1), (10), (11) and (12) the EFG approximation is obtained:

$$u^h(x) = \sum_{I=1}^{NP} \Psi_I(x) u_I \tag{13}$$

$\Psi_I(x)$ are shape functions having the expressions:

$$\Psi_I(x) = H^T(x) M^{[n]^{-1}}(x) B(x) \tag{14}$$

The choice of the weight function can be theoretically arbitrary as long as these meet some conditions. Synthetically, the most important conditions are: to be greater zero within the support domain; to be zero outside the support domain; to be monotonically decreasing from the point of interest; to be enough smooth, especially on the boundary.

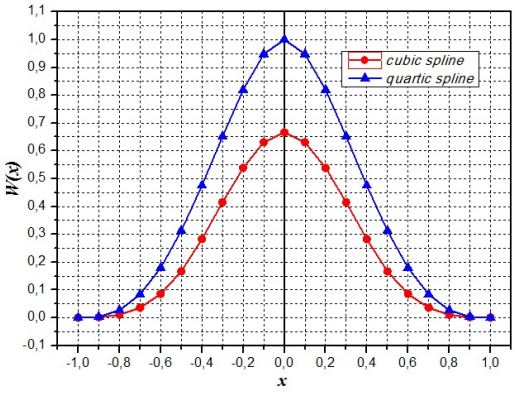

Fig. 3. Weight functions.

The most used weight functions are: the cubic and the quartic spline functions. In the Figure 3, a graphical representation of these weight functions is presented.

The EFGM matrix equation system

The moving least-squares approximation lacks the Kronecker delta function property. A weak-form formulation, including all the loads (on domain and on boundaries) is:

$$\int_\Omega \delta(Lu)^T D(Lu) d\Omega = \int_\Omega \delta u^T b d\Omega + \int_{\Gamma_t} \delta u^T \bar{t} d\Gamma + \delta \int_{\Gamma_u} \frac{1}{2}(u-\bar{u})^T \alpha (u-\bar{u}) d\Gamma \tag{15}$$

In the relation (15), the used notations, for a 2D problem, have the following forms and meaning: $u^T = \{u \quad v\}$ = displacement vector; $b^T = \{b_x \quad b_y\}$ = the body force vector; $\bar{t} = \sigma \cdot n$ = the prescribed traction on the boundary (Γ_t); n = the vector of unit outward normal at a point on boundary; $\bar{u} = u$ = the prescribed displacement on the boundary (Γ_u); $\alpha = [\alpha_1 \quad \alpha_2 \quad \ldots \quad \alpha_k]$ = is a diagonal matrix of penalty factors, where $k = 2$ for 2D and $k = 3$ for 3D; the penalty factors α_i can be function of coordinates (different from each other), but they have to be given;

practically, a constant large positive number is used;

$$\mathrm{D} = \frac{E}{1-\nu^2}\begin{bmatrix} 1 & \nu & 0 \\ \nu & 1 & 0 \\ 0 & 0 & \dfrac{1-\nu}{2} \end{bmatrix} = \text{matrix of material ; } \mathbf{L} = \begin{bmatrix} \dfrac{\partial}{\partial x} & 0 \\ 0 & \dfrac{\partial}{\partial y} \\ \dfrac{\partial}{\partial y} & \dfrac{\partial}{\partial x} \end{bmatrix} = \text{differential operator.}$$

Considering the fundamentals of the EFG method presented above, by their introducing in the relation (15), the following matrix equation is obtained,

$$\left[K + K^{\alpha}\right] \cdot U = F + F^{\alpha} \tag{16}$$

where K^{α} is the global penalty stiffness matrix and F^{α} is an additional force vector. In the case of using of the Lagrange multiplier method for essential boundary conditions, the relation (15) will be re-written and penalty factors a_i will be changed with Lagrange multiplayers λ, as it is shown in the relation (17).

$$\int_{\Omega} \left(L\delta u\right)^T \cdot \left(DLu\right) \cdot d\Omega = \int_{\Omega} \delta u^T \cdot b \cdot d\Omega + \int_{\Gamma_t} \delta u^T \cdot \overline{t} \cdot d\Gamma + \\ + \int_{\Gamma_u} \delta\lambda^T \cdot \left(u - \overline{u}\right) \cdot d\Gamma - \int_{\Gamma_u} \delta u^T \cdot \lambda \cdot d\Gamma \tag{17}$$

By a lot of mathematical transformation, by considering the relations of the EFG fundamentals, finally the following matrix equation is obtained,

$$\begin{bmatrix} K & G \\ G^T & 0 \end{bmatrix} \cdot \begin{bmatrix} U \\ \Lambda \end{bmatrix} = \begin{bmatrix} F \\ Q \end{bmatrix} \tag{18}$$

where K is the global stiffness matrix, G is the global stiffness matrix resulting from boundary conditions, U is the vector of the nodal parameters of the displacements, Λ is a vector collecting the nodal Lagrange multipliers for all field nodes on the boundaries, F is the global force vector and Q is the global vector of the forces resulting from the prescribed displacement on the boundary.

The equations (16) and (18) represent the final discretized system equations for the EFG method, using penalty method and Lagrange multiplier method, respectively. Solving of the equation (16) or (18) nodal parameters of the displacements are obtained; then, the nodal displacements u^h are obtained.

4. Illustrative example

The comparative analysis of the obtained results by FEM and by EFGM is performed for a simple problem which also has a theoretical solution. This simple problem consists in bending of a cantilever beam loaded at the end [5]. The calculus model of this problem is presented in Figures 4.

The calculus model is presented in the Figure 4, where $P = 2000N$; $l = 0.60m$; $E = 2 \cdot 10^{11} Pa$; $G = 0.76923 \cdot 10^{11} Pa$; $\upsilon = 0.30$; $h = 2c = 0.06m$; $c = 0.03m$; $b = 0.01m$.

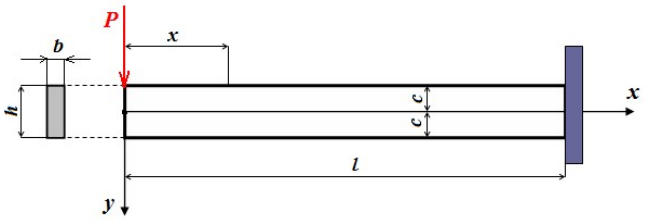

Fig. 4. Calculus model of the considered problem.

4.1. Analitical solution

The displacements u and v in any point of the beam is calculated with the relations (*Timoshenko, Theory of Elasticity, page. 38*):

$$u(x,y) = -\frac{Px^2 y}{2EI} - \frac{\upsilon P y^3}{6EI} + \frac{Py^3}{6GI} + \left(\frac{Pl^2}{2EI} - \frac{Pc^2}{2GI}\right)\cdot y \tag{19}$$

$$v(x,y) = \frac{\upsilon P x y^2}{2EI} + \frac{Px^3}{6EI} - \frac{Pl^2 x}{2EI} + \frac{Pl^3}{3EI} \tag{20}$$

Considering only the bending moment, the equation of deflection curve has the following form (*Timoshenko, Theory of Elasticity, page. 38*):

$$UY^M(x) = v(x)\Big|_{y=0} = \frac{Px^3}{6EI} - \frac{Pl^2 x}{2EI} + \frac{Pl^3}{3EI} \tag{21}$$

$$UY^M{}_{\max} = v_{\max} = v(x)\Big|_{y=0}^{x=0} = \frac{Pl^3}{3EI} \tag{22}$$

This relation is well known from elementary books on the strength of materials. By considering the influence of the shear forces the equation of the deflection curve becomes (*Timoshenko, Theory of Elasticity, page. 39*):

$$UY^{M+T}(x) = v(x)\Big|_{y=0} = \frac{Px^3}{6EI} - \frac{Pl^2 x}{2EI} + \frac{Pl^3}{3EI} + \frac{Pc^2}{2GI}(l-x) \tag{23}$$

$$UY^{M+T}{}_{\max} = v_{\max} = v(x)\Big|_{y=0}^{x=0} = \frac{Pl^3}{3EI} + \frac{Pc^2 l}{2GI} \tag{24}$$

Using the relations (22) and (24) the following values of maximum deflections of the beam are obtained: $UY^M_{\max} = 0.0040m$; $UY^{M+T}_{\max} = 0.004039m$

4.2. Numerical solutions

The numerical solutions, by FEM and by EFGM, were performed for five versions of discretization; these versions are presented bellow, in the Figure 5. Each of above tests has the following characteristics of the mesh:

- Test-1: FE dimension, 15x15 mm, having 4x40 = 160 FE, with 205 nodes;
- Test-2: FE dimension, 10x10 mm, having 6x60 = 360 FE, with 427 nodes;
- Test-3: FE dimension, 5x5 mm, having 12x120 = 1440 FE, with 1573 nodes;
- Test-4: FE dimension, 3.5x3.5 mm, having 17x172 = 2924 FE, with 3114 nodes;

- Test-5: FE dimension, 3x3 mm, having 20x200 = 4000 EF, with 4221 nodes.

The used finite element, both in FE analysis and EFG analysis, was the SHELL element with 4 nodes, in a plane-stress state.
The results are synthetically presented in the Table 1 and Table 2, for those two cases: only bending moment, respectively bending moment and shear force.
The Figures 6 and 7 present, in a graphic form, the evolution, according to the number of FE, of the maximum displacement *UY* and the errors of those two numerical method.
In the Figures 8 and 9, the influence of the considering of the shear forces is illustrated by graphical representation of the calculus errors of those two numerical method versus the number of finite elements.

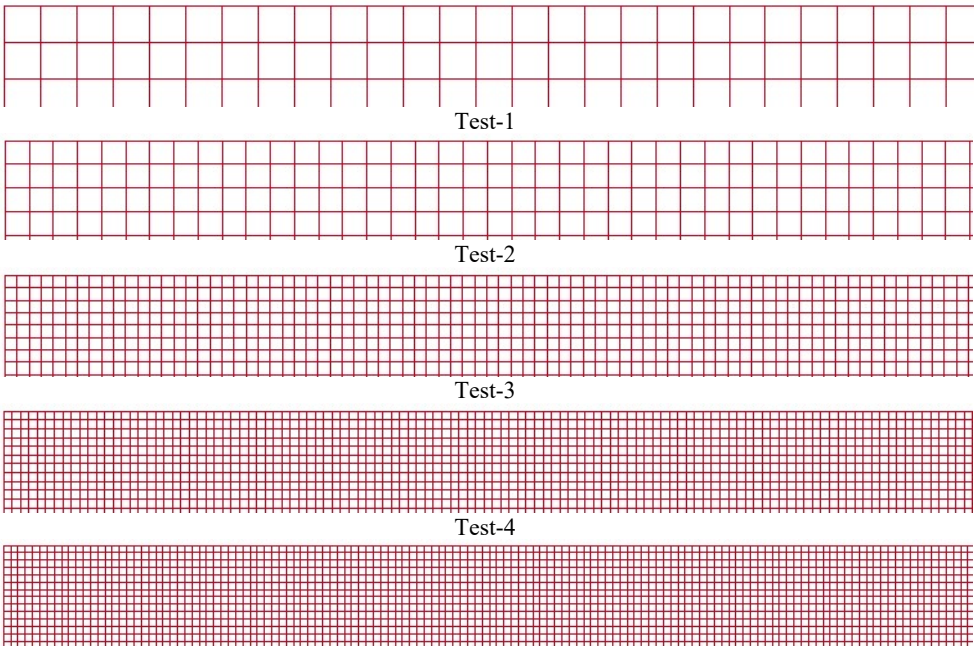

Fig. 5. Discretization versions of the structure.

Table 1. Maximum displacements under bending moment.

No. of F.E.	Analytical solution	FEM		EFGM	
	UY [m]	UY [m]	*Err. [%]*	UY [m]	*Err. [%]*
Test-1	0.004000	0,00428	*7,00*	0,003994	*-0,15*
Test-2		0,00414	*3,50*	0,004013	*0,33*
Test-3		0,00406	*1,50*	0,004026	*0,65*
Test-4		0,00405	*1,25*	0,004029	*0,72*
Test-5		0,00404	*1,00*	0,004029	*0,72*

Table 2. Maximum displacements under bending moment and shear force.

No. of F.E.	Analytical solution	FEM		EFGM	
	UY [m]	UY [m]	*Err. [%]*	UY [m]	*Err. [%]*
Test-1	0.004039	0,00429	*6,21*	0,003994	*-1,11*
Test-2		0,00415	*2,75*	0,004013	*-0,64*
Test-3		0,00407	*0,77*	0,004025	*-0,35*
Test-4		0,00406	*0,52*	0,004028	*-0,27*
Test-5		0,00406	*0,52*	0,004029	*-0,25*

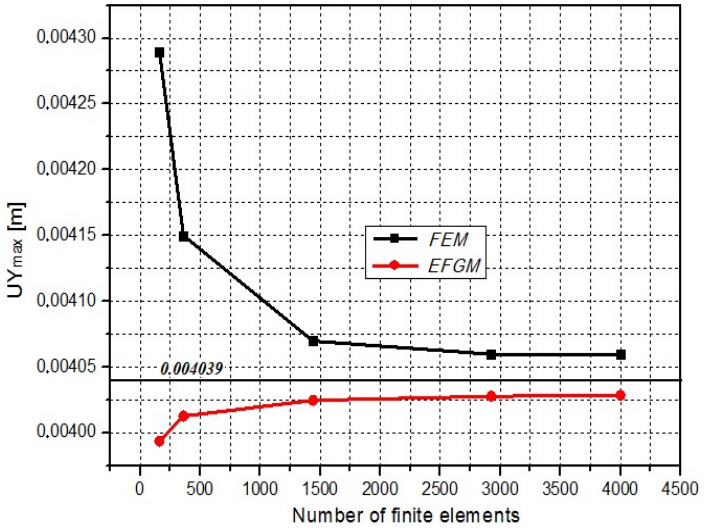

Fig. 6. Comparative graphical presentation of the maximum displacement.

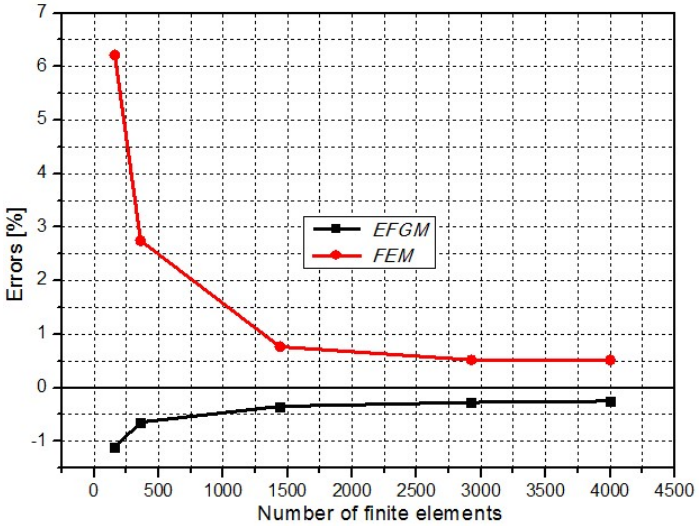

Fig. 7. Comparative graphical presentation of the errors.

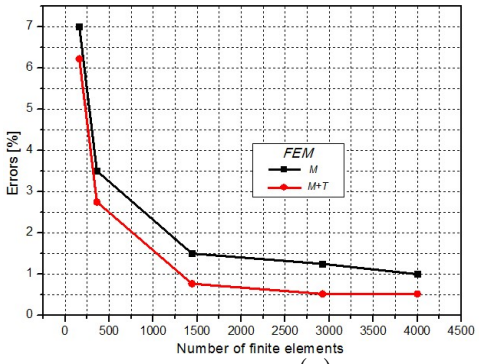

Fig. 8. The influence of the shear force (T) upon $UY_{\max}$ by FEM.

As the stress calculus is concerned very interesting observations can be made. Using the version of Test-3 a comparison between those three methods were made for the elements placed in the middle of the beam length, as the Figure 10 presents. The SX and SXY stresses values and their distributions were studied.

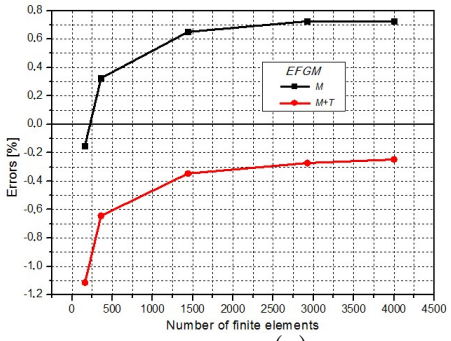

Fig. 9. The influence of the shear force (T) upon $UY_{\max}$ by EFGM.

The theoretical values of the stresses were calculated starting from relations (19) and (20) using Hooke's generalized law for the case of the plane stress state:

$$\varepsilon_x = \frac{\partial u}{\partial x} \tag{25}$$

$$\varepsilon_y = \frac{\partial v}{\partial y} \tag{26}$$

$$\gamma_{xy} = \frac{\partial v}{\partial x} + \frac{\partial u}{\partial_y} \tag{27}$$

$$SX \equiv \sigma_x = \frac{E}{1-\upsilon^2}\left(\varepsilon_x + \upsilon\varepsilon_y\right) \tag{28}$$

$$SXY \equiv \tau_{xy} = \frac{E}{2(1+\upsilon)} \cdot \gamma_{xy} \tag{29}$$

The values of SX and SXY stresses were calculated in the middle point of the selected elements (Fig. 10).

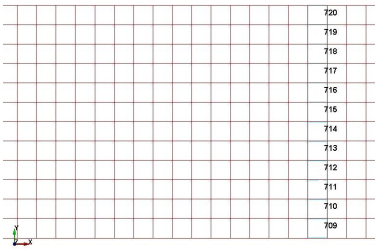

Fig. 10. Selected elements for graphical representation of the SX and SXY stresses.

Graphical representations of the SX and SXY stresses in the selected cross section (middle beam length) are presented in the Figures 11 and 12.

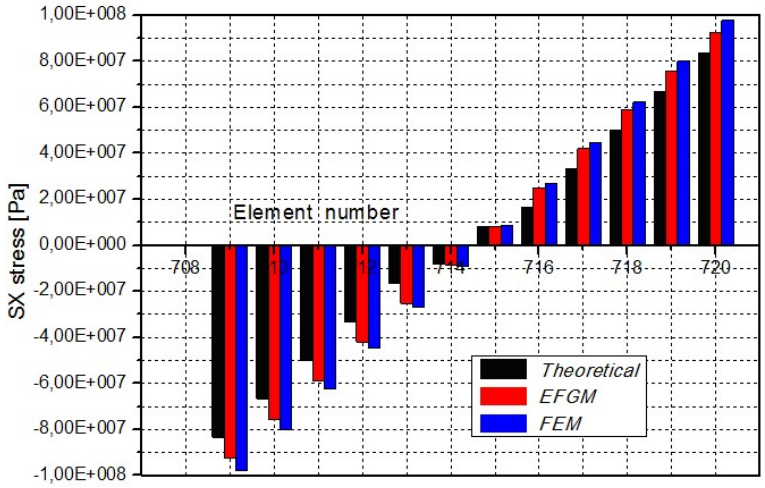

Fig. 11. The values of SX stresses on the selected elements calculated by those three methods.

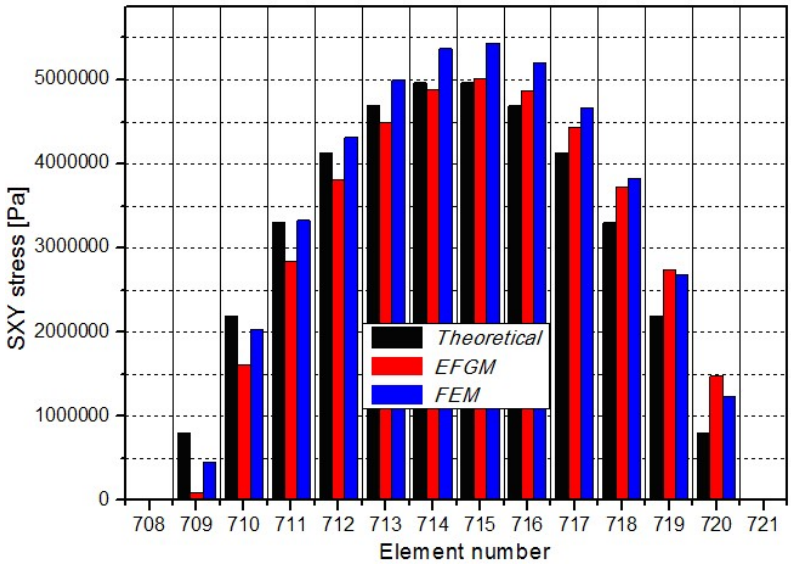

Fig. 12. The values of SXY stresses on the selected elements calculated by those three methods.

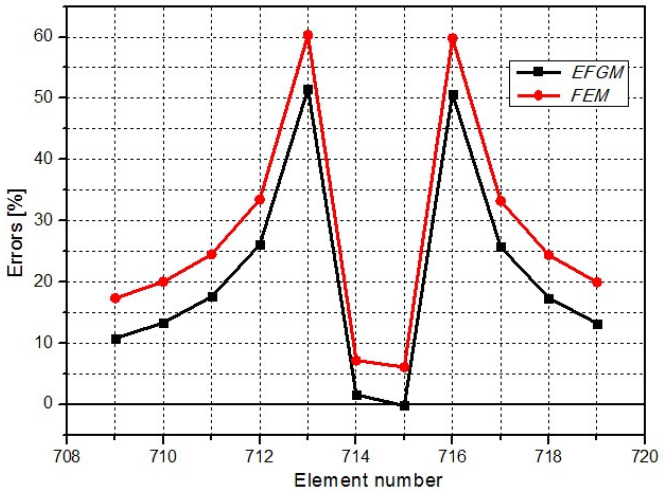

Fig. 13. Errors towards theoretical values for SX stresses.

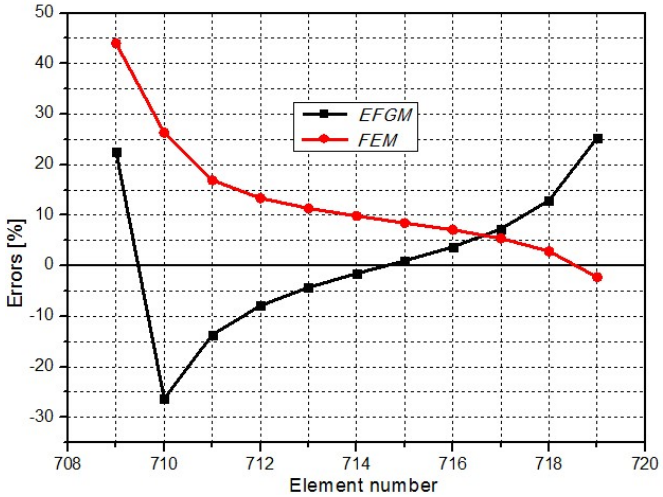

Fig. 14. Errors towards theoretical values for SXY stresses.

5. Conclusion

The study presented in this paper shows a part of our researching, which has and will have the aim to bring to the attention of specialists the using of this meshfree method – EFGM.

So, we presented in a comparative way, the calculus results because the best arguments for YES or NOT for a numerical method consist in quantitative determinations.

Unfortunately, by lacking enough space, we have referred only some aspects regarding those two numerical methods: FEM and EFGM. These aspects are the number of the finite elements, maximum displacements and the influence of the shear force upon calculus results.

Analyzing the quantitative values (Tables 1 and 2) and the graphical representations (Figures 6...9) some very important conclusions can be formulated.
So, the EFGM is more accurate, comparatively with FEM, in both cases: taking or not considering the influence of the shear forces.
The EFGM has a high convergence rate being more accurate than FEM.
By comparing those three methods (analytical method, FEM and EFGM) we can see that the EFGM is less sensitive with respect to the fine mesh (Figures 6 and 7).
Just in the case of the fewest elements (Test-1) the calculus error of the $UY_{\max}$ is under 1.50% using EFGM, as long as using FEM (Ansys code) the same error is over 6% (Fig. 7).
The convergence to the exact solution (analytical solution) is made from opposite directions (Figures 6 and 7) because of their approximation types: interpolation (FEM) and approximation (EFGM).
The influence of the shear force is a little one, but in some circumstances could have a significative influence and this is the reasons of our research.
Beginning with the Test-3, the errors, produced by considering of the shear force, go under 2% (Fig. 8). We could say that the EFGM is an effective method and it is found to be superior to FEM.
Similar conclusions can also be drawn on stresses SX and SXY (Figures 11 and 12); the values obtained by EFGM are closer to the theoretical values for the same point. This observation is valid for both SX and SXY stresses, for any point of the beam.
The errors along selected cross section presented in the Figures 13 and 14 are referring to the SX stress and SXY stress respectively; they are rather inadmissible, but they occur on a coarse mesh. Just in such conditions, the errors of the EFGM are under FEM errors. So, EFGM is more accurate than FEM.
This conclusion is based on many other arguments not presented here.
Some disadvantages, also not presented here, are to be going to be overpassed.
We consider that a right answer to the title question must be formulated by each user after studying and using of this meshfree method – EFGM.

References

[1] Li, G.R., *Meshfree Methods.Moving Beyond the Finite Element Method,* Second Edition, 2010 by Taylor and Francis Group, LLC, CRC Press.
[2] Liu G.R., Gu Y.T., *An Introduction to Meshfree Methods and Their Programming,* Published by Springer, P.O. Box 17, 3300 AA Dordrecht, The Netherlands, 2005 Springer.
[3] Năstăsescu V.A., Bârsan V., Iliescu N., *Upon Element-Free Galerkin Method and Its Using in Static and Dynamic Structure Analysis,* The 24th International Conference The Knowledge-Based Organization, Sibiu, 14-16 June 2018, p. 156-161.
[4] Shaofan Li, Wing Kam Liu, *Meshfree Particle Methods,* Springer-Verlag Berlin Heidelberg 2004, 2007.
[5] Timoshenko S., Goodier J.N., *Theory of Elasticity,* Second Edition, McGraw-Hill Book Company Inc., New-York, Toronto, London, 1951.